



Self-assembled monolayers of rigid thiols

Abraham Ulman^{a,*}, Jung F. Kang^{a,1}, Yitzhak Shnidman^{a,1}, Sheng Liao^{a,1},
Rainer Jordan^{a,1}, Gun-Young Choi^{a,1}, Julien Zaccaro^a,
Allan S. Myerson^a, Miriam Rafailovich^{b,1}, Jonathan Sokolov^{b,1},
Cathy Fleischer^c

^aDepartment of Chemical Engineering, Chemistry and Materials Science, Polytechnic University, Six Metrotech Center, Brooklyn, NY 11201, USA

^bDepartment of Materials Sciences and Engineering, State University of New York at Stony Brook, Stony Brook, NY 11794-2275, USA

^cImaging Support and Technology Division, Eastman Kodak Company, Rochester, NY 14650-2158, USA

Abstract

The preparation, structure, properties and applications of self-assembled monolayers (SAMs) of rigid 4-mercapto-biphenyls are briefly reviewed. The rigid character of the biphenyl moiety results in a molecular dipole moment that affects both the adsorption kinetics on gold surfaces, as well as the equilibrium structure of mixed SAMs. Due to repulsive intermolecular interaction, the Langmuir isotherm model does not fit the adsorption kinetics of these biphenyl thiols, and a new Ising model was developed to fit the kinetics data. The equilibrium structures of SAMs and mixed SAMs depend on the polarity of the solution from which they were assembled. Infrared spectroscopy suggests that biphenyl moieties in SAMs on gold have small tilt angles with respect to the surfaces normal. Wetting studies shows that surfaces of these SAMs are stable for months, thus providing stable model surfaces that can be engineered at the molecular level. Such molecular engineering is important for nucleation and growth studies. The morphology of glycine crystals grown on SAM surfaces depends on the structure of the nucleating glycine layer, which, in turn, depends on the H-bonding of these molecules with the SAM surface. Finally, the adhesion of PDMS cross-linked networks to SAM surfaces depends on the concentration of interfacial H-bonding. This non-linear relationship suggests that the polymeric nature of the elastomer results in a collective H-bonding effect. © 2000 Published by Elsevier Science B.V.

Keywords: Self-assembled monolayers; Rigid; Langmuir

* Corresponding author. Tel.: +1-718-260-3119; fax: +1-718-260-3125.

E-mail address: aulman@duke.poly.edu (A. Ulman).

¹NSF MRSEC for Polymers at Engineered Interfaces.

1. Introduction

Self-assembly is a spontaneous coordinated action of independent entities to produce a larger structure. This is a phenomenon of great importance from biology (embryology and morphogenesis) to chemistry (the formation of supramolecular structures from small molecules), and even to robotics, where the objective is to produce and program a group of micro-robots that are capable of self-assembly. For the purpose of nanofabrication, building nanostructures and nanoelectronic devices, self-assembly is envisaged as an important avenue for fabricating and employing supramolecular nanostructures with useful properties. Building blocks of such structures may be polymers, DNA and proteins, nanoparticles and surfactants (Fig. 1). However, for these components to self-assemble to design functional units they must form strong attractive interactions at their interfaces (Kuhn and Ulman, 1995). It is the understanding of how such interfaces can be designed that is the foundation of the work described in this review.

During the past fifteen years, great progress has been made in the preparation of self-assembled monolayers (SAMs) (for reviews on self-assembled monolayers see Ulman, 1991, 1996, for a review on SAMs on thiols see Ulman, 1999). SAMs are highly ordered and oriented and can incorporate a wide range of groups both in the alkyl chain and at the chain termina. Therefore, a

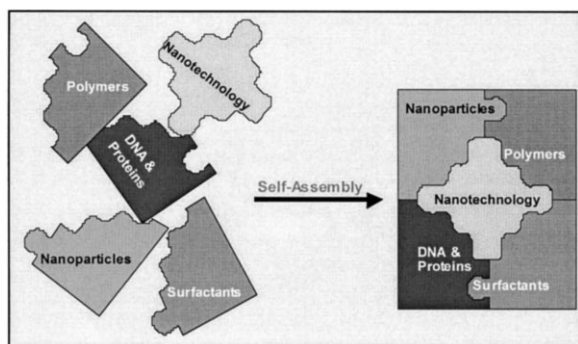


Fig. 1. Polymers, DNA and proteins, nanoparticles and surfactant molecules may form spontaneously supramolecular assemblies if strong interfacial interactions exist.

variety of surfaces with specific interactions can be produced with fine structural control (Ulman et al., 1991), producing surface energies that span the range from ‘Teflon-like’ surfaces (surface CF_3 groups) to very high-energy surfaces (surface OH or COOH groups), e.g. surface tensions of 10–70 dyne cm^{-1} . That interfacial interaction can be designed using SAMs has been shown in studies of molecular recognition (Spinke et al., 1993; Motesharei and Myles, 1994; Mrksich et al., 1995), biomaterial interfaces (Mrksich and Whitesides, 1996; Yousaf and Mrksich, 1999), cell growth (Tidwell et al., 1997; Chen et al., 1998; Houseman and Mrksich, 1998), crystallization (Zaccaro et al., 2000) and many other systems (Bishop and Nuzzo, 1996). The shortcoming of SAMs made of flexible alkyl derivatives, however, is that thermal disorder results in surface-gauche defects, and thus surface disorder. Studies of sum-frequency vibration spectroscopy show that the structure of a surface is clearly perturbed when it interacts strongly with another condensed phase (Ong et al., 1992), alerting us that structural perturbations need to be considered. This is especially serious for very polar surface groups, such as OH (Evans et al., 1991), where the introduced disorder may be significant (Hautman and Klein, 1991; Hautman et al., 1991; Kacker et al., 1997) and not confined to the surface (Evans et al., 1991). Therefore, a preferred system will be one in which conformational disorder has been eliminated, as completely as possible. This can be achieved by using rigid molecules, where surface functional groups have no conformational freedom and are ‘stuck’ at the surface.

The idea to use biphenyl thiols resulted from a study we carried out on 4,4'-dioctylbiphenyl, which spontaneously forms stable suspended liquid crystal (SLC) films (Young et al., 1978). The results suggest that 4'-substituted-4-mercapto-biphenyl derivatives (Fig. 2) may form ordered SAMs on Au(111) surfaces (Ulman and Scaringe, 1992). Beyond their rigidity, the advantage of these aromatic thiols is the conjugation between the adsorbing thiolate and the 4'-substituent. This conjugation affects the acidity of the thiol proton, and hence may make the thiolate a softer or a harder ligand (Pearson and Songstad, 1967;

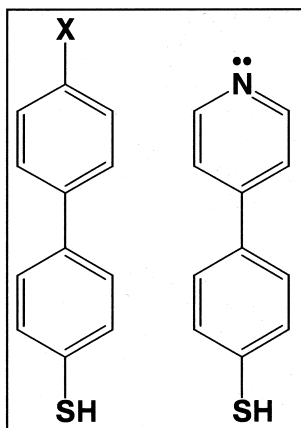


Fig. 2. 4-Mercaptobiphenyls and 4(4'-mercaptophenyl)pyridine.

Pearson, 1968). Since the thiolate is an electron-donating group, an electron attracting substituent will result in a significant molecular dipole moment. Dipolar interactions may alter adsorption kinetics (Liao et al., 2000) and the composition of mixed SAMs in equilibrium (Kang et al., 1998, 1999a) as became apparent from studies that will be described briefly in this review.

Sabatani et al. (1993) assembled thiophenolate, 4-mercaptobiphenyl, and 4-mercaptoterphenyl onto gold, and reported that the latter two formed reproducible SAMs that were substantially more stable than those from mercaptophenol, presumably due to greater intermolecular interactions. Using molecular mechanics calculations they predicted a herringbone structure for the adsorbed 4-mercaptoterphenyl with molecules oriented close to the surface normal. Recent molecular dynamics simulations in our group confirmed this structure, and suggested tilt angles of $\leq 15^\circ$ (Wong et al., unpublished results).

Sita and colleagues have examined a related set of compounds where acetylenic units were located between the phenyl rings (Dhirani et al., 1996; Zehner and Sita, 1997; Zehner et al., 1999). Using scanning tunneling microscopy (STM), they observed the formation of ordered domains for the species on gold. The data provided the first evidence for the formation of an ordered SAM that is not based on an *n*-alkanethiol derivative and was consistent with the calculated structure

for 4-mercaptoterphenyl on gold (Akiyama et al., 1996). Tour and colleagues have synthesized an expanded collection of phenyl, biphenyl, and terphenyl derivatives, both with, and without acetylenic units that link the phenyl rings, and characterized SAMs derived from them (Tour et al., 1995; Jones et al., 1997; Pearson and Tour, 1997). They suggested using rigid, conjugated molecules as molecular conductors, and Sachs et al. (1997) measured the rates of interfacial electron transfer through similar systems prepared by Hsung et al. (1995a,b). Finally, Tao et al. (1997) applied cyclic voltammetry (CV) to study the structure of aromatic-derivatized thiol monolayer on gold. They showed that for phenyl-substituted thiols, the stability of a monolayer formed on gold depended on the location of the benzene ring in the alkyl chain, as well as on the length of this chain.

2. Adsorption kinetics

We have examined biphenyl thiols with different substituents at the 4-position [$X = \text{SCH}_3$, $\text{N}(\text{CH}_3)_2$, CH_3 , CF_3 , and NO_2] (Ong et al., 1992). These substituents may be divided into electron acceptor (NO_2 , CF_3), and electron donor [$\text{N}(\text{CH}_3)_2$, SCH_3 , CH_3] groups. The electron density on the adsorbing thiol S-atom should be smaller for the 4'- NO_2 - than, for example, for the 4'- $\text{N}(\text{CH}_3)_2$ -substituent. Four or five different concentrations were used for each thiol. For all concentrations, no multilayers could be detected by ellipsometry, and film thickness at the end of the experiment was between 14 ± 1 and 15 ± 1 Å. Fig. 3 shows thiol concentration dependence of adsorption kinetics of $\text{CH}_3\text{S-Ph-Ph-SH}$, indicating that the mass equilibrium was reached after a period of few minutes, clearly *slower* than reported adsorption kinetics for *n*-alkanethiols (Karpovich and Blanchard, 1994).

Most researchers agree that the process of adsorption of thiols onto gold can be divided into two or three steps, the first is fast, and the following steps are much slower (Buck et al., 1992; Hähner et al., 1993; McCarley et al., 1993). Thus, it takes less than 10 s to finish the first step

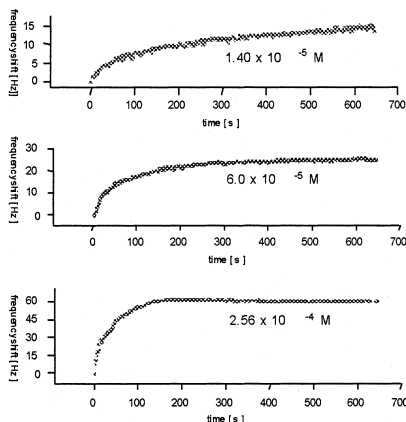


Fig. 3. Concentration dependence of adsorption kinetics for $\text{CH}_3\text{S-Ph-Ph-SH}$.

(sulfur adsorption), and 10 h to complete the second step (orientation ordering). The kinetics of the first step probably is a mixture of physical and chemical adsorption processes — which cannot be separated — that is governed by the surface-head group interaction, while that of the orientation-ordering step is governed by the inter-chain interactions. The QCM studies, however, can provide information on the first, adsorption step. Detailed information on the orientation and

ordering step will require, for example, sum-frequency generation studies.

We compared two different models to fit the quartz crystal microbalance (QCM) data. The first is the Langmuir isotherm model (Fig. 4 red line) that assumes that there is no strong interaction between adsorbates. Karpovich and Blanchard applied successfully this model to fit the adsorption kinetics of alkanethiols on gold (Karpovich and Blanchard, 1994). However, as is apparent from Fig. 4 this may not be the case for polar 4-mercaptobiphenyl molecules.

In the Langmuir model, $d\theta/dt = k_a(1 - \theta)C - k_d\theta$, where θ is the coverage, C the concentration, and k_a and k_d are the adsorption and desorption kinetic constants, respectively. We defined Err as the deviation of fitted coverage from experimental data as:

$$Err = \left[1/n_t \sum_{i=1}^{n_t} (\theta_f(t_i) - \theta_e(t_i))^2 \right]^{1/2} \quad (1)$$

where $\theta_f(t_i)$ is the fitted coverage at time t_i , $\theta_e(t_i)$ is the experimental coverage [$\theta_e(t_i) = \Delta f(t_i)/\Delta f_{\max}$ where $\Delta f(t_i)$ is the frequency shift at time t_i and Δf_{\max} is the final maximum fre-

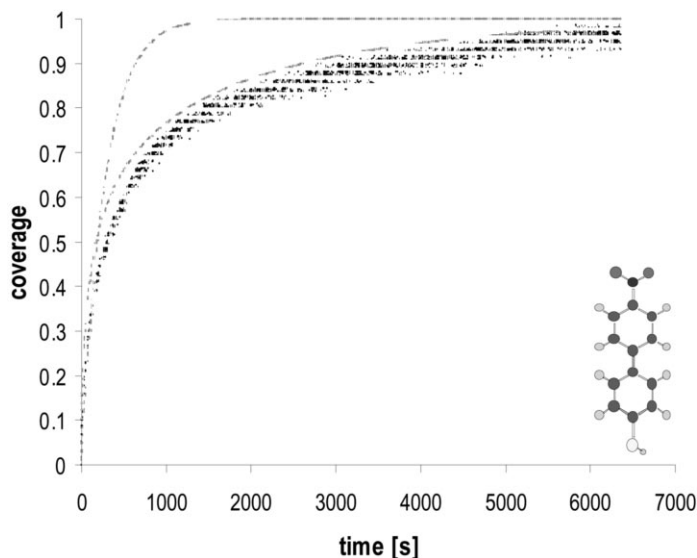


Fig. 4. Fitting comparison using two different models for adsorption of 4'-nitro-4' mercaptobiphenyl on gold.

Table 1

Err values for Langmuir fits of QCM data for the adsorption of different 4-mercaptobiphenyls on gold

4-Mercaptobiphenyl	k_a	k_d	<i>Err</i>
NO ₂ -Ph-Ph-SH	27	6.3×10^{-5}	0.106
CF ₃ -Ph-Ph-SH	148	1.1×10^{-4}	0.103
N(CH ₃) ₂ -Ph-Ph-SH	191	1.7×10^{-4}	0.087
CH ₃ -Ph-Ph-SH	212	1.6×10^{-4}	0.093
CH ₃ S-Ph-Ph-SH	736	9.6×10^{-4}	0.073

quency shift], and n_i is the total number of data points. Table 1 gives the result summary of the Langmuir fit. It shows that the biggest deviation from the Langmuir isotherm model (largest *Err* value) occurs when the 4'-position of 4-mercaptobiphenyl is substituted with an NO₂ group. On the other hand, when the 4'-position is CH₃S, there is the smallest deviation from the Langmuir isotherm model (*Err* has the smallest value). Fig. 5 shows the observed adsorption kinetics, k_{obs} , as a function of concentration of 4'-methylmercapto-4-mercaptobiphenyl in toluene. Notice that even for the least polar molecule there is no linear relationship as typical for the Langmuir adsorption mechanism. Considering that 4'-nitro-4-mercaptobiphenyl has the largest dipole moment and 4'-methylmercapto-4-

mercaptobiphenyl has the smallest dipole among these five molecules, Table 1 and Figs. 4 and 5 suggest that the interaction between adsorbing molecules have to be taken into account, and the Langmuir isotherm does not fit well in this case.

Thus, a new chemisorption model that takes inter-adsorbate interactions into consideration explicitly was developed. The process of chemisorption of 4-mercaptobiphenyls from solution to the (111) gold surface was modeled as follows. We assume that:

1. the energy of the single, isolated adsorbed molecule is lowered by μ_s (where $\mu_s > 0$) relative to the energy of the molecule in the bulk solution;
2. adsorbed molecules occupy the sites of a triangular lattice on the (111) surface of gold, and molecules occupying nearest-neighbor sites on that lattice have a pair interaction-energy of $-\varepsilon$; and
3. there is an energy barrier of ω for adsorption and $\omega + \mu$ for desorption of single, isolated molecules to and from the surface.

Under these assumptions, the energy of the 4-mercaptobiphenyl molecules adsorbed to the

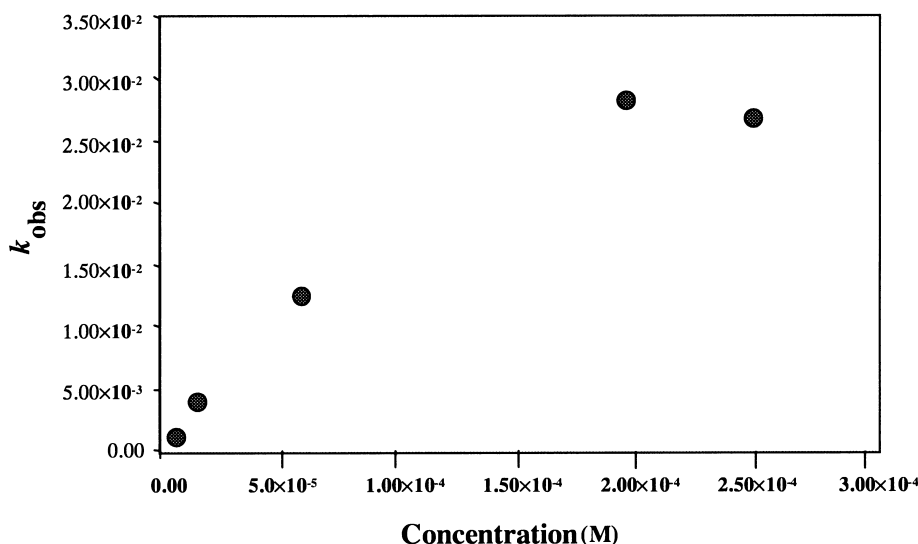


Fig. 5. A plot of k_{obs} vs. concentration of 4'-methylmercapto-4-mercaptobiphenyl in toluene.

Au(111) surface is approximated by following the lattice-gas Hamiltonian, defined on the triangular lattice:

$$H = -1/2\varepsilon \sum_{\vec{r}} \sum_{i=1}^z t_{\vec{r}} t_{\vec{r}+\hat{e}_i} - \mu_s \sum_{\vec{r}} t_{\vec{r}} \quad (2)$$

where $t_{\vec{r}} = 1, 0$ denotes that the site \vec{r} is occupied or empty, respectively. Here $z = 6$ is the number of nearest-neighbors at each site (coordination number) for the triangular surface lattice of adsorption sites. Using $t_{\vec{r}} = (1 + s_{\vec{r}})/2$, where $s_{\vec{r}} = \pm 1$ are Ising pseudo-spins denoting occupied (empty) sites, the lattice-gas Hamiltonian above is equivalent (up to an energy constant) to an Ising Hamiltonian

$$H = -1/8\varepsilon \sum_{\vec{r}} \sum_{i=1}^z s_{\vec{r}} s_{\vec{r}+\hat{e}_i} - (\frac{1}{2}\mu_s + \frac{1}{4}z\varepsilon) \sum_{\vec{r}} t_{\vec{r}} \quad (3)$$

We represent adsorption from solution as a Glauber (spin-flip) stochastic dynamic process. The transition rate for this process is assumed to be of the simple form $\varphi(\lambda) = \exp(-\lambda/2)$, where $\lambda = \Delta H_{\pm}/k_B T$ is the change in energy associated with the adsorption or desorption of a molecule at a single site, scaled by $k_B T$, the thermal energy. This satisfies the local detailed balance condition $\varphi(\lambda) = e^{-\lambda} \varphi(-\lambda)$, thus assuring convergence to equilibrium at long times. Assuming translational invariance for the mean site occupancy, $\langle t_{\vec{r}} \rangle = n_{\vec{r}} \equiv n$, the time evolution of n is obtained from the master equation within a dynamic mean field approximation, as follows:

$$\frac{1}{\Gamma} \frac{dn}{dt} = (1-n)n_b \exp[(z\tilde{\varepsilon}n + \tilde{\mu}_s)/2] - n(1-n_b) \exp[-(z\tilde{\varepsilon}n + \tilde{\mu}_s)/2] \quad (4)$$

where $\tilde{\mu}_s = \mu_s/k_B T$, $\tilde{\varepsilon} = \varepsilon/k_B T$, and n_b is the bulk solution occupancy, related to the bulk concentration by $n_b = v_m c_b$, where v_m is a molecular volume. Here, Γ has the dimensions of inverse time $\Gamma = 1/\tau$, where τ is some microscopic relaxation time. At specified temperature T and bulk concentration c_b , the mean surface site occupancy (coverage) can be calculated by a numerical

integration of Eq. (5), if the three parameters μ_s , ε and Γ are known. Note that (a) if $\varepsilon = 0$, we recover the Langmuir adsorption equation and (b) at equilibrium, $dn/dt = 0$. Assuming $n_b \ll 1$, this leads to the following equation determining equilibrium surface occupancy n_{eq}

$$(1 - n_{eq})n_b \exp[(z\tilde{\varepsilon}n_{eq} + \tilde{\mu}_s)/2] - n_{eq}(1 - n_b) \exp[-(z\tilde{\varepsilon}n_{eq} + \tilde{\mu}_s)/2] = 0 \quad (5)$$

or

$$(1 - n_{eq})n_b - n_{eq}(1 - n_b) \times \exp[-(z\tilde{\varepsilon}n_{eq} + \tilde{\mu}_s)] = 0 \quad (6)$$

We have performed least-square fits of the three parameters μ_s , ε and Γ in Eq. (4) to relative coverage data obtained from QCM measurements. This was done by minimizing a cumulative square-error objective function obtained from the differences between mean site occupancies numerically integrated from Eq. (4) and the experimental QCM relative coverage time sequences. Each fit used data from a series of two to four experiments performed at the same temperature, and using the same adsorbates and solvents but two to four different bulk concentrations of the adsorbents.

Fig. 4 shows a comparison between the Langmuir and the new model fits for the adsorption kinetics of 4'-nitro-4-mercaptobiphenyl on gold in toluene. Fitting parameters for the adsorption kinetics of 4-mercaptobiphenyl derivatives are presented in Table 2. We can see the fits are much improved, and the *Err* values are significantly smaller than those in Table 1.

3. SAM Structure

Fourier transform infrared spectra (FTIR) of all 4'-substituted-4-mercaptobiphenyls and their SAMs were studied in transmission mode for a KBr pellet of the solid and in the external reflection (ER) mode for the SAMs on gold and silver,

Table 2

Fitting of QCM data for the adsorption of different 4-mercaptobiphenyls on gold to the new adsorption model

4-Mercaptobiphenyl	ρ^0	$ \Delta\sigma $	<i>Err</i>	Γ (s ⁻¹)	ε (kcal/mol)	μ_s (kcal/mol)
NO ₂ -Ph-Ph-SH	0.81	0.87	0.064	0.0071	-2.44	10.10
CF ₃ -Ph-Ph-SH	0.53	0.59	0.025	0.0145	-2.29	12.20
N(CH ₃) ₂ -Ph-Ph-SH	-0.32	0.26	0.048	0.0217	-1.95	12.39
CH ₃ -Ph-Ph-SH	-0.14	0.08	0.065	0.0310	-1.21	11.98
CH ₃ S-Ph-Ph-SH	-0.06	0	0.031	0.155	-1.08	11.41

respectively. Fig. 6 represents the ERFTIR spectra of 4'-trifluoromethyl-4-mercaptobiphenyl in KBr, in CCl₄ solution (5 mM), and in a SAM on gold. The simplification of the spectrum in the SAM environment reflects the perpendicular orientation of the biphenyl moiety. This suggests that the surface-S-C angle should be $\leq 180^\circ$, which is in agreement with theoretical calculations (Sellers et al., 1993). There it was suggested that depending on molecular interactions the hybridization of the S-atom might be either sp or sp³. Further support for this structure comes from helium and X-ray diffractions studies.

Fig. 7 shows the FTIR spectrum of the same SAM in Fig. 6, but prepared from a toluene solution. Contrary to the tilt of alkyl chain in SAMs of alkanethiolates on gold, which is driven by the reestablishment of interchain van der Waals attraction, the more perpendicular molecular orientation in SAMs of mercaptobiphenyl derivatives is probably the result of maximizing interactions. However, when the molecule possesses a strong dipole moment, intermolecular interactions results in repulsion and instability, and thus the tilt angle may strongly depend on the polarity of the solvent from which the SAM

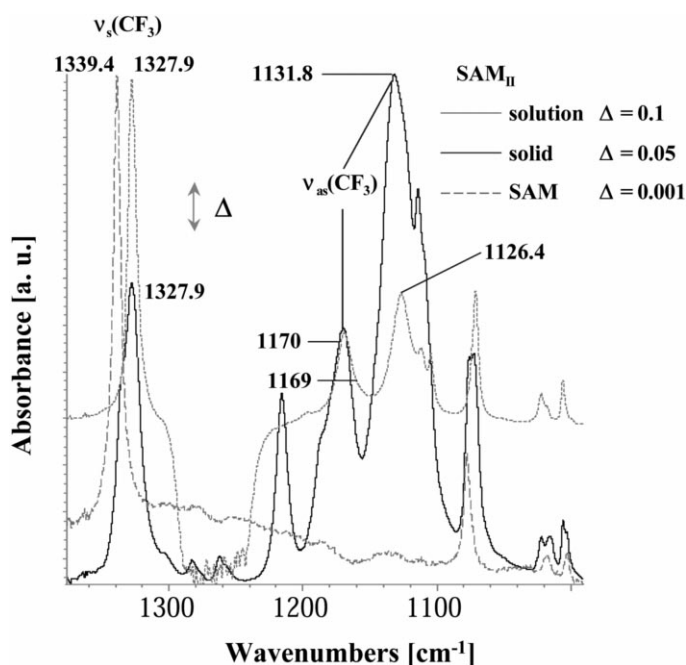


Fig. 6. The ERFTIR spectra of 4'-trifluoromethyl-4-mercaptobiphenyl in KBr, in CCl₄ solution (5 mM), and in a SAM on gold prepared in ethanol.

was prepared. This becomes even more pronounced in the case of mixed SAMs.

When mixed SAMs of 4'-trifluoromethyl-4-mercaptobiphenyl and 4'-methyl-4-mercaptobiphenyl were prepared from ethanol (Fig. 8), the position of both the symmetric CF_3 -vibration [$\nu_s(\text{CF}_3)$] and the b_{1u} biphenyl skeletal modes showed a linear relationship with surface CF_3 group concentration. The $\nu_s(\text{CF}_3)$ peak shift was explained by a classical electromagnetic theory, and an excellent agreement between theory and experiments was obtained (Kang et al., 1999b).

However, when the same mixed SAMs were prepared from toluene, the maximum shift in the $\nu_s(\text{CF}_3)$ peak position was smaller (5.2 vs. 8.9 cm^{-1}), and the peak intensities revealed a clear development of a plateau. Fig. 9 shows the integrated area under the $\nu_s(\text{CF}_3)$ band for mixed CF_3 : CH_3 SAMs made in toluene and ethanol vs. the molar fraction of the 4'- CF_3 -4-mercaptobiphenyl in solution. This plateau suggests that there is a significant driving force for mixing, explained by the fact that the two components have molecular dipole in opposite directions with respect to the surface. The question was then is the driving

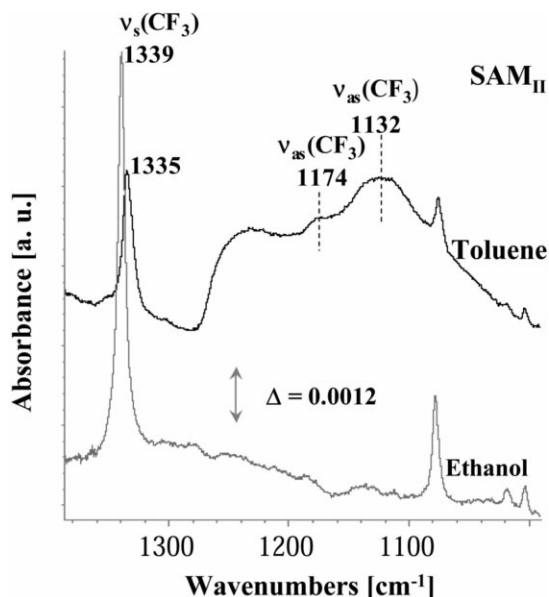


Fig. 7. The ERFTIR spectra of 4'-trifluoromethyl-4-mercaptobiphenyl SAM on gold prepared from ethanol and from toluene solutions.

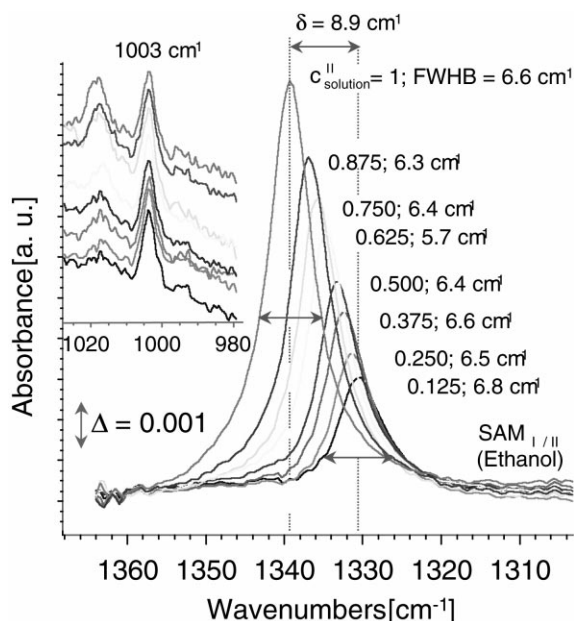


Fig. 8. The $\nu_s(\text{CF}_3)$ band for mixed SAMs of 4'-trifluoromethyl-4-mercapto-biphenyl and 4'-methyl-4-mercaptobiphenyl made in ethanol. The insert shows a common band at 1000 cm^{-1} .

force for mixing strong enough to facilitate thiol exchange. Indeed, it was found that when either SAMs were placed in a 10 M solution of the other component, equilibrium was established after 43 h, resulting in mixed SAMs with approximately the same composition (Fig. 10). This driving force for mixing should depend on the dipole moments of the two components, and should increase with the increasing dipole, due to the increased intermolecular repulsion in the pure SAMs.

Fig. 11 shows that intermolecular repulsion in a SAM of 4'-nitro-4-mercaptobiphenyl is so significant, that there is a driving force for dilution with 4'-methylmercapto-4-mercaptobiphenyl, which for all practical purposes does not have a molecular dipole. In fact, even when mixed SAMs were prepared in toluene solutions with 90% concentration of the 4'-nitro-4-mercaptobiphenyl, its surface concentration was only $\sim 50\%$. These mixed SAMs allow, for the first time, a systematic control of surface dipole concentration.

When mixed SAMs of 4'-nitro-4-mercaptobiphenyl and 4'-dimethylamino-4-mercapto-

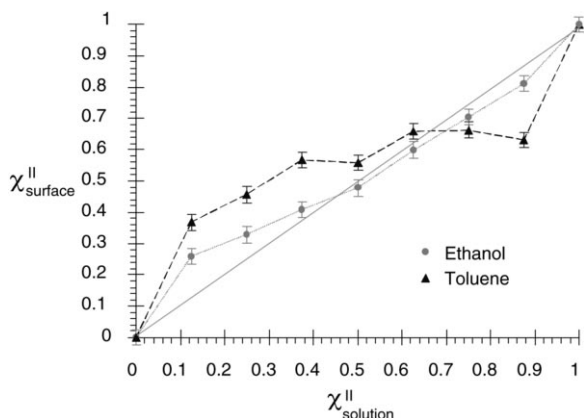


Fig. 9. Integrated area under the $s(\text{CF}_3)$ band for mixed $\text{CF}_3:\text{CH}_3$ SAMs made in toluene and ethanol vs. the molar fraction of the 4'- CF_3 -4-mercaptobiphenyl in solution.

biphenyl were prepared in toluene, the surface NO_2 , as determined by external reflection Fourier transform infrared (ER-FTIR) spectroscopy, showed a plateau at 40% NO_2 surface concentration (Fig. 11). This can be explained by assuming that the equilibrium concentration of the two components in the mixed SAM, in a non-polar solvent, is driven by the formation of a two-dimensional assembly with zero net dipole moment. Using the idea that the Hammett equation (March, 1977) may be applicable in these systems,

one can express the dipole moment of the SAM as a sum of contributions:

$$(1 - X)(\text{NO}_2) + X(\text{N}(\text{CH}_3)_2) = 0$$

Where $=_p(\text{NO}_2 \text{ or } \text{N}(\text{CH}_3)_2) -_p(\text{S}-\text{Au})$, assuming that the molecular dipole of the two thiols result primarily from the substitution at the 4- and 4'-positions. To account for the contribution of the S-Au to the dipole moment the $_p^+$ value for SCH_3 (-0.164) was selected (Kang et al., 1999b). If the effect of electronic state on dipole moment of the para-substituted compound is considered to be simply additive (Debye, 1931; Debe, 1982), $(\text{NO}_2) = 0.942$, and $(\text{N}(\text{CH}_3)_2) = -0.666$, and Eq. (2) gives $X = 0.4$, well within the experimental result.

4. Stable model surfaces

Fig. 12 shows a plot of Cos of advancing and receding water contact angles on mixed CH_3/OH surfaces. These surfaces were prepared by assembling mixed SAMs of 4'-methyl-4-mercaptobiphenyl and 4'-hydroxy-4-mercaptobiphenyl on gold. The small contact angle hysteresis ($\leq 5^\circ$), attributed to the high quality of the annealed gold surfaces, is unusually small. Furthermore, when

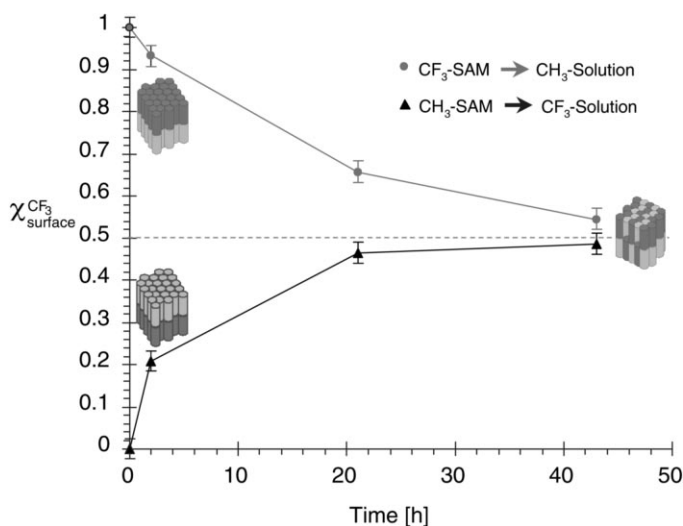


Fig. 10. Integrated area under the $s(\text{CF}_3)$ band for the exchange experiments.

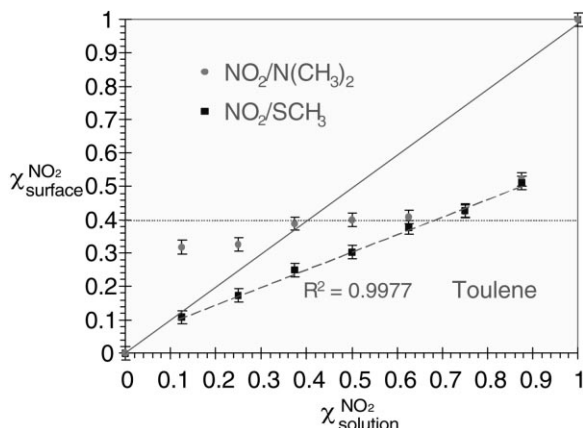


Fig. 11. Integrated area under the $\nu(\text{NO}_2)$ band for mixed SAMs[NO_2/SCH_3] and SAMs[$\text{NO}_2/\text{N}(\text{CH}_3)_2$] made in toluene vs. the molar fraction of NO_2 in solution.

the same samples were investigated after 1-month storage under nitrogen, the same contact angles were recorded. Such stability makes these surfaces ideal for studies of surface and interfacial phenomena. In the following, we report on experiments where engineered surfaces were used as substrates.

5. Surface-initiated polymerization

Traditionally, polymer brushes have been pre-

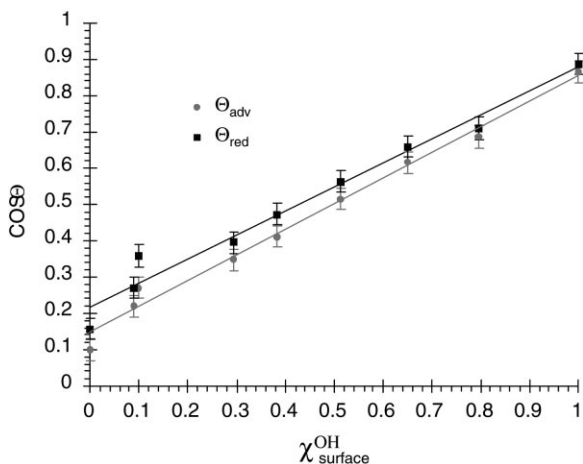


Fig. 12. Cos of advancing and receding water contact angles on mixed CH_3/OH surfaces.

pared by (a) selective physisorption of block-copolymers from bulk or solution onto a solid surface, where a shorter ‘anchor’ block adsorbs strongly onto the surface, leaving the remaining ‘buoy’ block tethered to the interface (Hadziioannou et al., 1983; Dan and Tirrell, 1993; Belder et al., 1997). (b) Chemical grafting or chemisorption of polymer chains onto a reactive surface via a terminal-coupling group (Häussling et al., 1991; Zhao et al., 1994). However, both techniques have their limitation in terms of the maximum grafting density that can be obtained. It is easy to picture that an already adsorbed chain screens still available grafting sites in its vicinity, because a tethered polymer chain tries to maintain its random coil conformation. As the grafting density increases, the chains have to increasingly stretch to allow further grafting, which results in a decrease of the rate of grafting kinetics (Dorgan et al., 1993; Dijt et al., 1994a,b). At some point, a limiting situation is reached that is dominated by the free energies of stretching, chain-chain interactions, and solvation. Hence, the grafting density of a brush, formed by the traditional ‘transplanting’ methods, is self-limiting.

SAMs of tethered biphenyllithium moieties (Fig. 13) were used to initiate anionic polymerization of styrene on gold substrates (Jordan et al., 1999). ER-FTIR spectra of the resulting polymer layer (Fig. 14) confirm a successful reaction, and

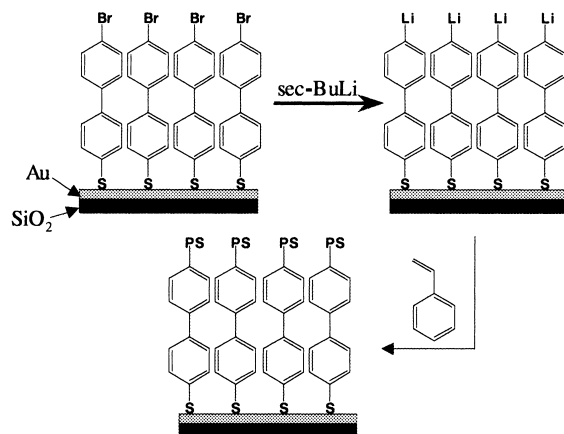


Fig. 13. Surface-initiated living anionic polymerization of styrene using rigid lithiated biphenyl SAM surfaces as initiator.

furthermore indicate preferred orientation of the grafted polystyrene chains. The thickness of the layer was estimated by ellipsometry to be between 18 and 20 nm. AFM studies revealed a smooth homogeneous polymer surface through the substrate with a roughness of 3–5 Å (rms). Spin-coated polystyrene films dewet immediately upon annealing, to give polymer droplets on top of the polystyrene brush, with contact angles of 2–5°. Swelling experiments, using toluene as the good solvent, and ellipsometry as the analytical tool, suggest surface grafting density of 7–8 chains/Rg²; a value never attained before using the conventional polymer adsorption techniques. With the expected arrival of the new TOF-SIMS in our MRSEC, we expect to obtain direct information on the molecular weight and its distribution.

6. Nucleation and growth of glycine crystals

Silane SAMs have been used to promote heterogeneous nucleation and growth of iron hydroxide crystals (Tarasevich et al., 1996) and to study the effect of surface chemistry on calcite nucleation, attachment and growth (Archibald et al., 1996). The crystallization of CaCO₃ was investi-

gated on surfaces of alkanethiolate SAMs on gold (Küther and Tremel, 1997), and recently it was reported that SAMs of functionalized alkanethiols could control the oriented growth of calcite (Aizenberg et al., 1999). The heterogeneous nucleation and growth of malonic acid (HOOCCH₂COOH) was investigated using alkanethiolate SAMs on gold that terminated with carboxylic acid and with methyl groups (Frostman et al., 1994).

We selected SAMs and mixed SAMs of 4'-hydroxy-4-mercaptobiphenyl, and 4'-methyl-4-mercaptobiphenyl on gold (111) surfaces to serve as templates for the nucleation and growth of glycine crystals. This is because we were interested in the effect of H-bonding on the packing and ordering of the nucleating layer. It was found that glycine nucleates in the α -glycine structure independent of OH surface concentration, but that crystal morphology depends on the composition of the nucleating SAM surface (Fig. 15). The crystallographic planes corresponding to the nucleation surfaces, for the different SAM surfaces under study, were determined by interfacial angle measurements. For nucleation on 100% OH surfaces, the glycine crystallographic plane corresponding to the nucleation is {011}, whereas for

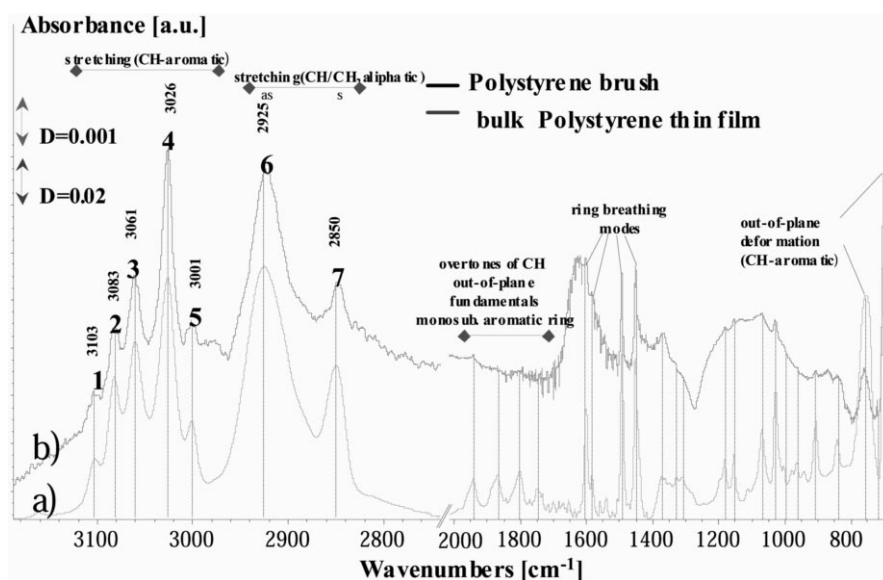


Fig. 14. ERFTIR spectra of bulk and brush polystyrene.

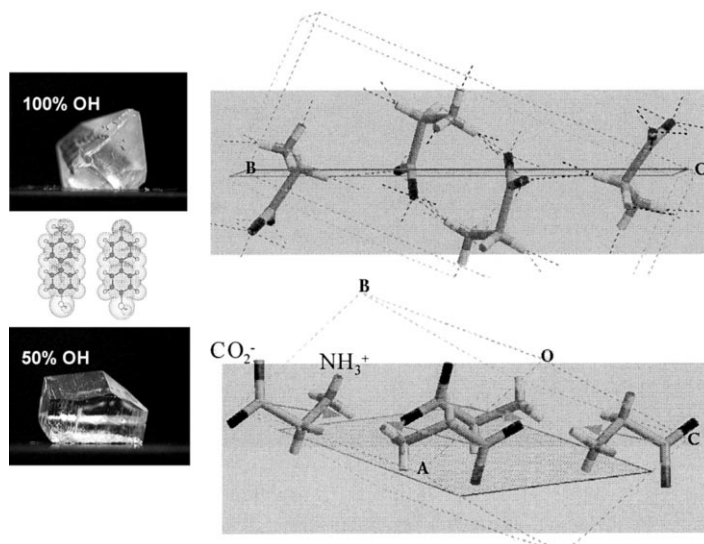


Fig. 15. Proposed molecular structure of the nucleation planes of glycine on 100% OH SAM (top), and on 50% OH and 100% CH₃ (bottom) surfaces.

the 0 and 50% OH surfaces, the crystallographic plane corresponding to the nucleation surface is a {h0l} face, probably {101}.

7. Adhesion studies

We have used SAMs to study the effect of acid–base interactions on the adhesion between solid surfaces (Choi et al., 1999). An increase in adhesion to poly(dimethylsiloxane) (PDMS) cross-linked networks was observed in the order of increasing acidity of surface OH protons [Au/(CH₂)₁₁OH < Au/S(C₆H₄)₂OH < Au/S(CH₂)₁₅-COOH < Au/S(CH₂)₁₁PO(OH)₂]. To systematically control surface OH concentration, we used the mixed OH/CH₃ SAMs shown in Fig. 16. We observed that the strength of adhesion is proportional to the number of surface OH groups but that the relationship is highly non-linear (Fig. 13), probably due to the collective nature of H-bonding between the PDMS chain and surface OH groups.

8. Conclusions

The preparation, structure, properties and ap-

plications of self-assembled monolayers (SAMs) of rigid 4-mercaptobiphenyls are briefly reviewed. The rigid character of the biphenyl moiety results in a molecular dipole moment that affects both the adsorption kinetics on gold surfaces, as well as the equilibrium structure of mixed SAMs. Due

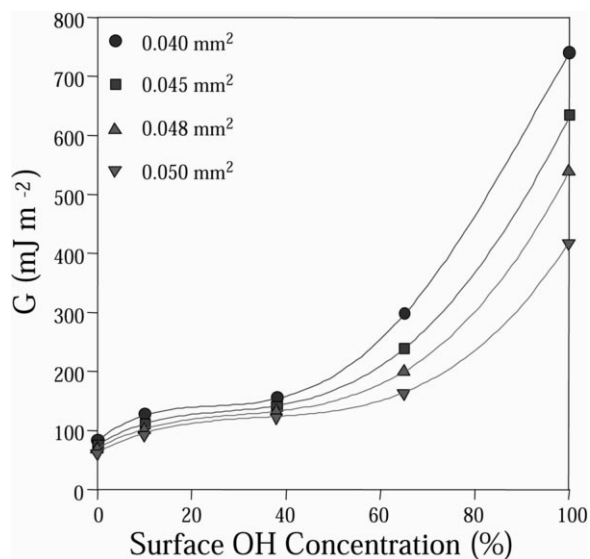


Fig. 16. Plots of G with respect to surface OH concentrations for different contact areas.

to repulsive intermolecular interaction, the Langmuir isotherm model does not fit the adsorption kinetics of these biphenyl thiols, and a new Ising model was developed to fit the kinetics data. The equilibrium structures of SAMs and mixed SAMs depend on the polarity of the solution from which they were assembled. Infrared spectroscopy suggests that biphenyl moieties in SAMs on gold have small tilt angles with respect to the surfaces normal. Wetting studies shows that surfaces of these SAMs are stable for months, thus providing stable model surfaces that can be engineered at the molecular level. Such molecular engineering is important for nucleation and growth studies. The morphology of glycine crystals grown on SAM surfaces depends on the structure of the nucleating glycine layer, which, in turn, depends on the H-bonding of these molecules with the SAM surface. Finally, the adhesion of PDMS cross-linked networks to SAM surfaces depends on the concentration of interfacial H-bonding. This non-linear relationship suggests that the polymeric nature of the elastomer results in a collective H-bonding effect.

References

- Aizenberg, J., Black, A.J., Whitesides, G.M., 1999. *J. Am. Chem. Soc.* 121, 4500.
- Akiyama, T., Imahori, H., Ajawakom, A., Sakata, Y., 1996. *Chem. Lett.* 907–908.
- Archibald, D.D., Qadri, S.B., Gaber, B.P., 1996. *Langmuir* 12, 538.
- Belder, G.F., ten Brinke, G., Hadziioannou, G., 1997. *Langmuir* 13, 4102 (and references therein).
- Bishop, A.R., Nuzzo, R.G., 1996. *Curr. Opin. Colloid Interface Sci.* 1, 127.
- Buck, M., Grunze, M., Eiser, F., Fiser, J., Trger, F., 1992. *J. Vac. Sci. Technol. A* 10, 926–929.
- Chen, C.S., Mrksich, M., Huang, S., Whitesides, G.M., Ingber, D.E., 1998. *Biotechnol. Progr.* 14, 356.
- Choi, G.Y., Kang, J.F., Ulman, A., Zurawsky, W., 1999. *Langmuir* 15.
- Dan, N., Tirrell, M., 1993. *Macromolecules* 26, 4310.
- Debe, M.K., 1982. *Appl. Surf. Sci.* 14, 1.
- Debye, P., 1931. *The Dipole Moment and Chemical Structure*. London and Glasgow, Blackie & Son Limited.
- Dhirani, A.-A., Zehner, R.W., Hsung, R.P., Guyot-Sionnest, P., Sita, L.R., 1996. *J. Am. Chem. Soc.* 118, 3319–3320.
- Dijt, J.C., Stuart, M.A.C., Fleer, G.J., 1994a. *Macromolecules* 27, 3207.
- Dijt, J.C., Stuart, M.A.C., Fleer, G.J., 1994b. *Macromolecules* 27, 3219.
- Dorgan, J.R., Stamm, M., Toprakcioglu, C., JÈrÙme, R., Fetters, L.J., 1993. *Macromolecules* 26, 5321.
- Evans, S.D., Sharma, R., Ulman, A., 1991. *Langmuir* 7, 156.
- Frostman, L.M., Bader, M.M., Ward, M.D., 1994. *Langmuir* 10, 576.
- Hadziioannou, G., Patel, S., Granick, S., Tirrell, M., 1983. *Macromolecules* 108, 2869.
- Hähner, G., Wöll, C.h., Buck, M., Grunze, M., 1993. *Langmuir* 9, 1955.
- Häussling, L., Knoll, W., Ringsdorf, H., Schmitt, F.J., Yang, J., 1991. *Makromol. Chem., Macromol. Symp.* 46, 145.
- Hautman, J., Klein, M.L., 1991. *Phys. Rev. Lett.* 67, 1763.
- Hautman, J., Bareman, J.P., Mar, W., Klein, M.L., 1991. *J. Chem. Soc. Faraday Trans.* 87, 2031.
- Houseman, B.T., Mrksich, M., 1998. *J. Org. Chem.* 63, 7552.
- Hsung, R.P., Babcock, J.R., Chidsey, C.E.D., Sita, L.R., 1995a. *Tetrahedron Lett.* 36, 4525.
- Hsung, R., Chidsey, C.E.D., Sita, L.R., 1995b. *Organometallics* 14, 4808.
- Jones II, L., Schumm, J.S., Tour, J.M., 1997. *J. Org. Chem.* 62, 1388.
- Jordan, R., Ulman, A., Kang, J.F., Rafailovich, M., Sokolov, J., 1999. *J. Am. Chem. Soc.* 121, 1016.
- Küther, J., Tremel, W., 1997. *Chem. Commun.* 2029.
- Kacker, N., Kuman, S.K., Allara, D.L., 1997. *Langmuir* 13, 6366.
- Kang, J.F., Liao, S., Jordan, R., Ulman, A., 1998. *J. Am. Chem. Soc.* 120, 9662.
- Kang, J.F., Ulman, A., Liao, S., Jordan, R., 1999a. *Langmuir* 15, 2095.
- Kang, J.F., Jordan, R., Kurth, D.G., Ulman, A., 1999b. *Langmuir* 15, 5555.
- Karpovich, D.S., Blanchard, G.J., 1994. *Langmuir* 10, 3315.
- Kuhn, H., Ulman, A., 1995. *Thin Films*. In: Ulman, A. (Ed.), *Supramolecular Assemblies: Vision and Strategy*, vol 20. Academic Press, Boston.
- Liao, S., Ulman, A., Shnidman, Y., 2000. *J. Am. Chem. Soc.* 122, 0000.
- March, J., 1977. *Advanced Organic Chemistry — Reactions, Mechanism, and Structure*, 2nd edition New York, McGraw-Hill Book Company.
- McCarley, R.L., Dunaway, D.J., Willicut, R.J., 1993. *Langmuir* 9, 2775.
- Motesharei, K., Myles, D.C., 1994. *J. Am. Chem. Soc.* 116, 7413.
- Mrksich, M., Whitesides, G.M., 1996. *Annu. Rev. Biophys. Biomol. Struct.* 25, 55.
- Mrksich, M., Grunwell, J.R., Whitesides, G.M., 1995. *J. Am. Chem. Soc.* 117, 12009.
- Ong, T.H., Ward, R.N., Davies, P.B., Bain, C.D., 1992. *J. Am. Chem. Soc.* 114, 6243.
- Pearson, R.G., 1968. *J. Chem. Educ.* 45, 581–643.
- Pearson, R.G., Songstand, J., 1967. *J. Am. Chem. Soc.* 89, 1827.

- Pearson, D.L., Tour, J.M., 1997. *J. Org. Chem.* 62, 1376.
- Sabatani, E., Cohen-Boulakia, J., Bruening, M., Rubinstein, I., 1993. *Langmuir* 9, 2974.
- Sachs, S.B., Dudek, S.P., Chidsey, C.E.D., 1997. *J. Am. Chem. Soc.* 119, 10563.
- Sellers, H., Ulman, A., Shnidman, Y., Eilers, J.E., 1993. *J. Am. Chem. Soc.* 115, 9389.
- Spinke, J., Liley, M., Guder, H.-J., Angermaier, L., Knoll, W., 1993. *Langmuir* 9, 1821.
- Tao, Y.T., Wu, C.C., Eu, J.Y., Lin, W.L., 1997. *Langmuir* 13, 4018.
- Tarasevich, B.J., Rieke, P.C., Liu, J., 1996. *Chem. Mater.* 8, 292.
- Tidwell, C.D., Ertel, S.I., Ratner, B.D., Tarasevich, B.J., Atre, S., Allara, D.L., 1997. *Langmuir* 13, 3404.
- Tour, J.M., Jones II, L., Pearson, D.L. et al., 1995. *J. Am. Chem. Soc.* 117, 9529.
- Ulman, A., Scaringe, R., 1992. *Langmuir* 8, 894.
- Ulman, A., Evans, S.D., Shnidman, Y., Sharma, R., Eilers, J.E., Chang, J.C., 1991. *J. Am. Chem. Soc.* 113, 1499.
- Ulman, A., 1991. *An Introduction to Ultrathin Organic Films.* Academic Press, Boston.
- Ulman, A., 1996. *Chem. Rev.* 96, 1533.
- Ulman, A. (Ed.), 1999. *Thin Films*, vol. 23. Academic Press, Boston.
- Wong, J., Shnidman, Y., Ulman, A. Unpublished results.
- Young, C.Y., Pindak, R., Clark, N.A., Meyer, R.B., 1978. *Phys. Rev. Lett.* 40, 773.
- Yousaf, M.N., Mrksich, M., 1999. *J. Am. Chem. Soc.* 121, 4286.
- Zaccaro, J., Kang, J.F., Ulman, A., Myerson, A., 2000. *Langmuir* 16, 0000.
- Zehner, R.W., Sita, L.R., 1997. *Langmuir* 13, 2973.
- Zehner, R.W., Pearson, B.F., Hsung, R.P., Sita, L.R., 1999. *Langmuir* 15, 1121.
- Zhao, W., Krausch, G., Rafailovich, M.H., Sokolov, J., 1994. Lateral structure of a grafted polymer layer in a poor solvent. *Macromolecules* 27, 2933.